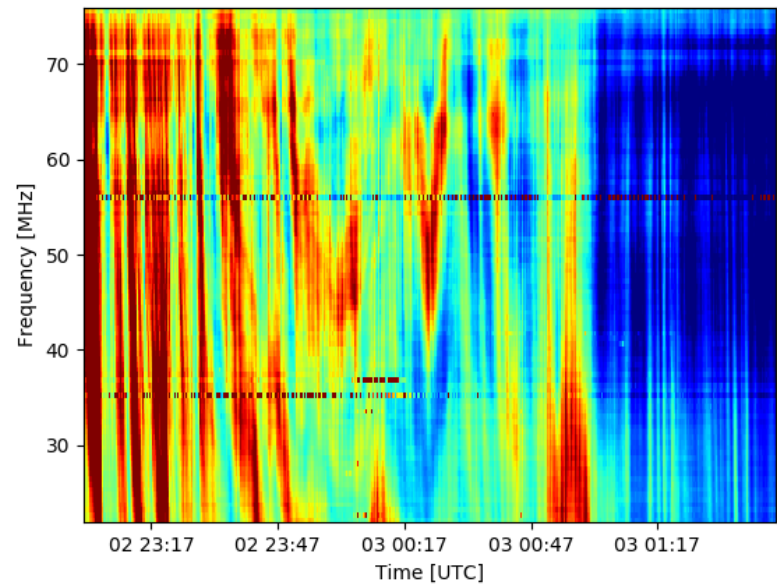
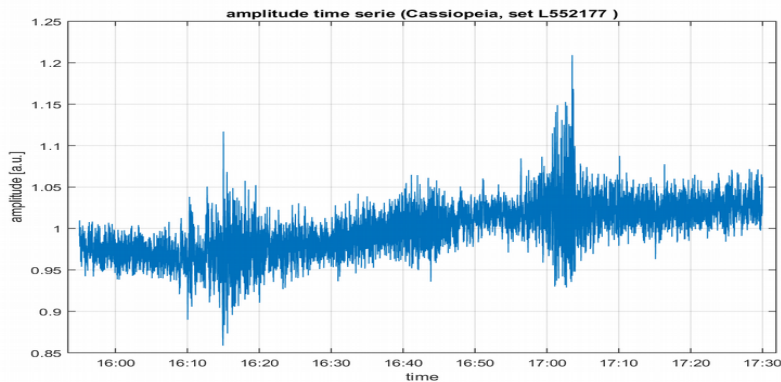
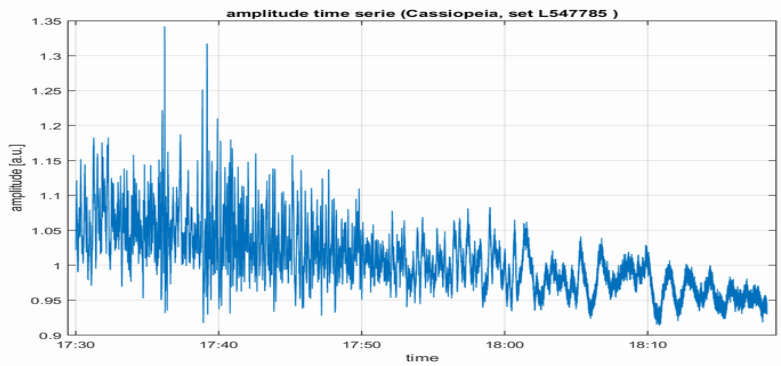
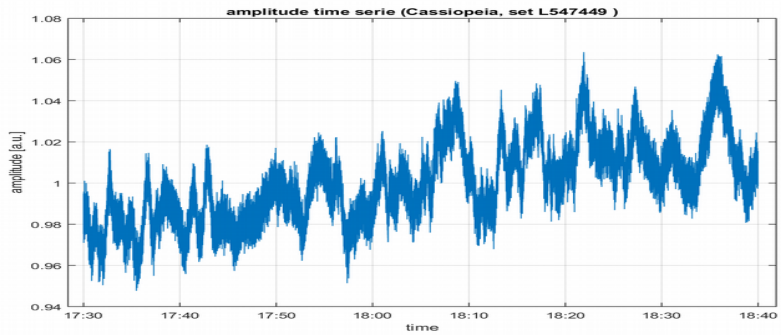
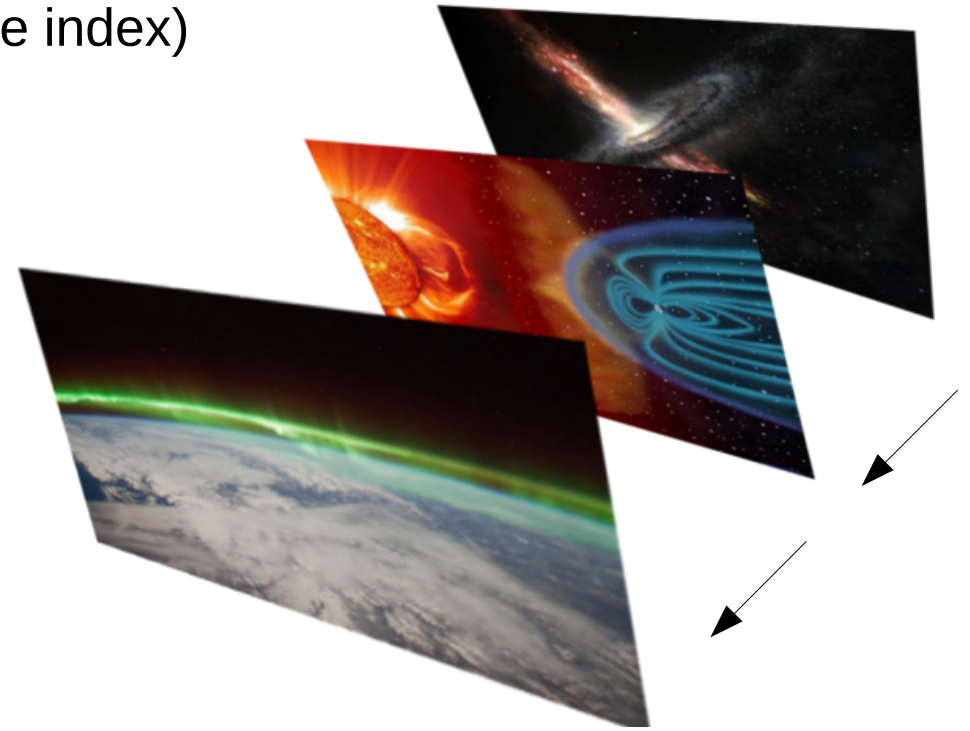


Spatio-temporal analysis of LOFAR scintillation measurements

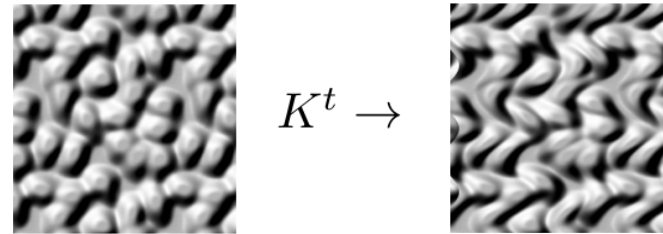
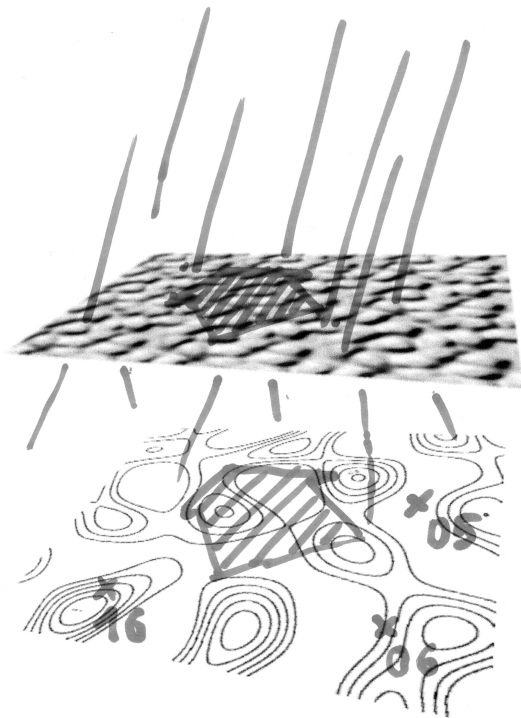
M. Grzesiak, D. Przepiórka, M. Pożoga, B. Matyjasiak,
H. Rothkaehl, K. Budzińska and R. Wronowski

Scintillation

(fluctuations of wave characteristics after passing through medium with variable refractive index)



Modeling pattern evolution – dispersion analysis



$$\psi(\mathbf{r}, t) = \int d\mathbf{r}' K^t(\mathbf{r} - \mathbf{r}') \psi(\mathbf{r}', 0)$$

$$\hat{\psi}(\mathbf{k}, t) = \hat{\psi}(\mathbf{k}, 0) e^{\Omega(\mathbf{k})t}$$

$$\mathbb{E}[\psi(\mathbf{r}_1, t_1) \psi(\mathbf{r}_2, t_2)] = \int d\mathbf{k} P(\mathbf{k}) e^{\Omega(\mathbf{k})\tau} e^{i\mathbf{k} \cdot \boldsymbol{\zeta}} = C(\boldsymbol{\zeta}, \tau),$$

$$\boldsymbol{\zeta} = \mathbf{r}_2 - \mathbf{r}_1, \tau = t_2 - t_1$$

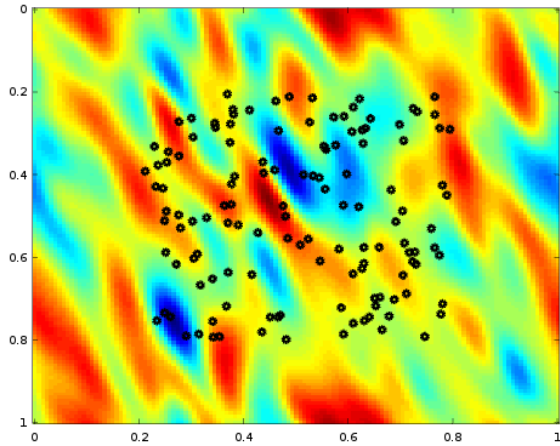
$$P(\boldsymbol{\zeta}, \omega) = \int d\tau C(\boldsymbol{\zeta}, \tau) e^{i\omega\tau} = \int d\tau e^{-i\omega\tau} \int d\mathbf{k} P(\mathbf{k}) e^{\Omega(\mathbf{k})\tau} e^{i\mathbf{k} \cdot \boldsymbol{\zeta}} =$$

$$\int d\mathbf{k} P(\mathbf{k}) e^{i\mathbf{k} \cdot \boldsymbol{\zeta}} \delta(\omega - \Omega(\mathbf{k}))$$

$$\langle \boldsymbol{\zeta} \rangle = \frac{\int d\boldsymbol{\zeta} \boldsymbol{\zeta} C(\boldsymbol{\zeta}, \tau)}{\int d\boldsymbol{\zeta} C(\boldsymbol{\zeta}, \tau)}$$

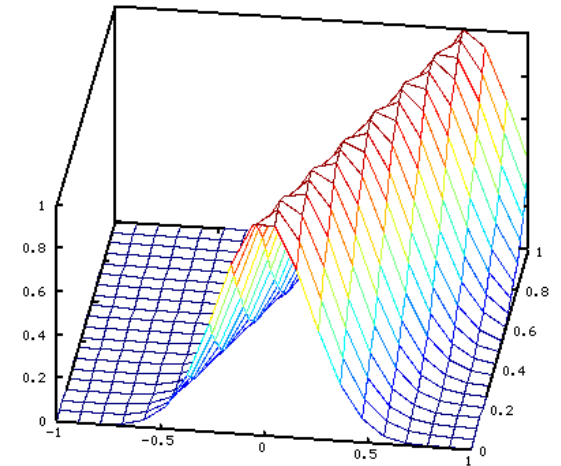
$$\frac{\partial}{\partial \tau} \langle \boldsymbol{\zeta} \rangle = \nabla_{\mathbf{k}} \Omega(\mathbf{k})|_{\mathbf{k}=0}$$

Basic example – rigid motion



$$K(\mathbf{r}' - \mathbf{r}, t) = \delta(\mathbf{r}' - (\mathbf{r} - \mathbf{v}dt))$$

$$\frac{\partial}{\partial t} C - \mathbf{v} \cdot \nabla_{\xi} C = 0$$



$$\xi_{\alpha} = \mathbf{r}_k - \mathbf{r}_l$$

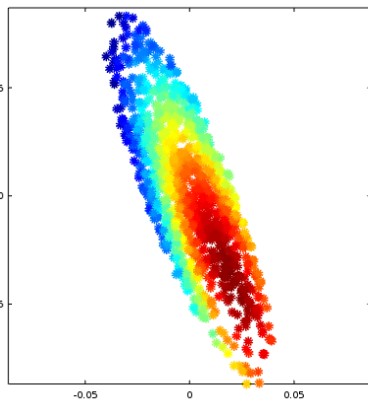
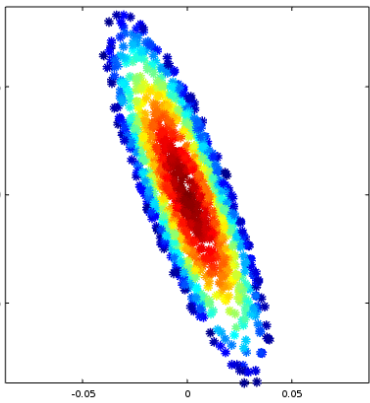
Simulation

Example from LOFAR

$$\tau_{\alpha} = 0$$

<

$$\tau_{\alpha}$$



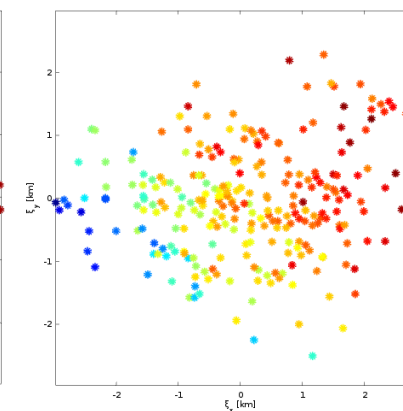
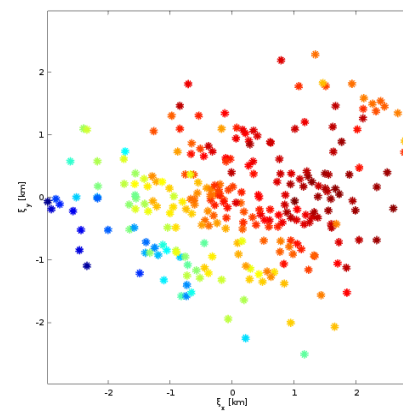
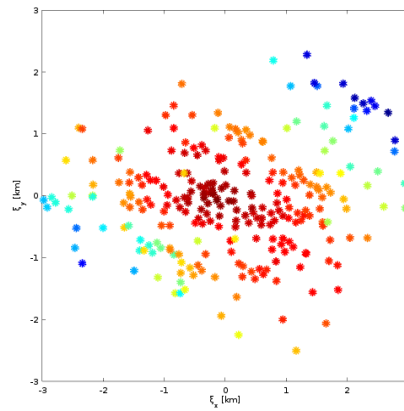
$$\tau_{\alpha} = 0$$

<

$$\tau_{\alpha}$$

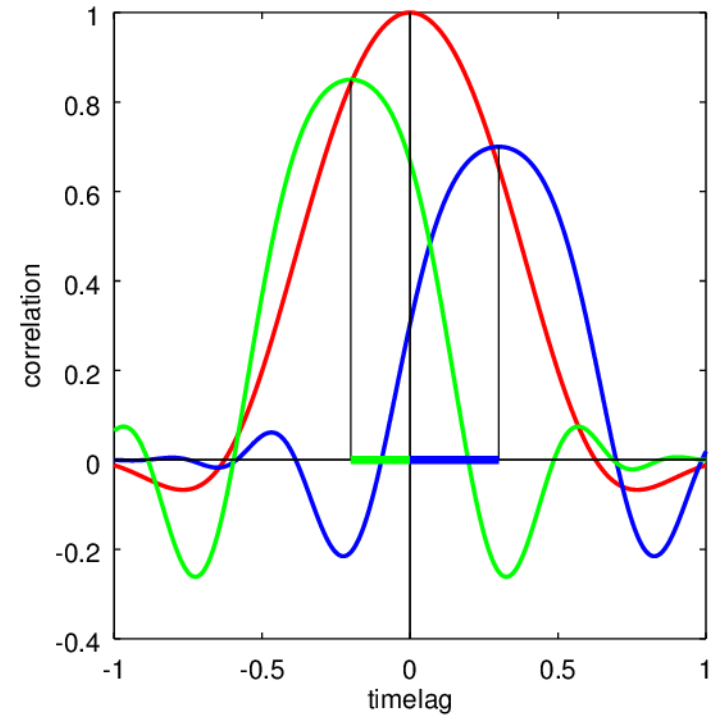
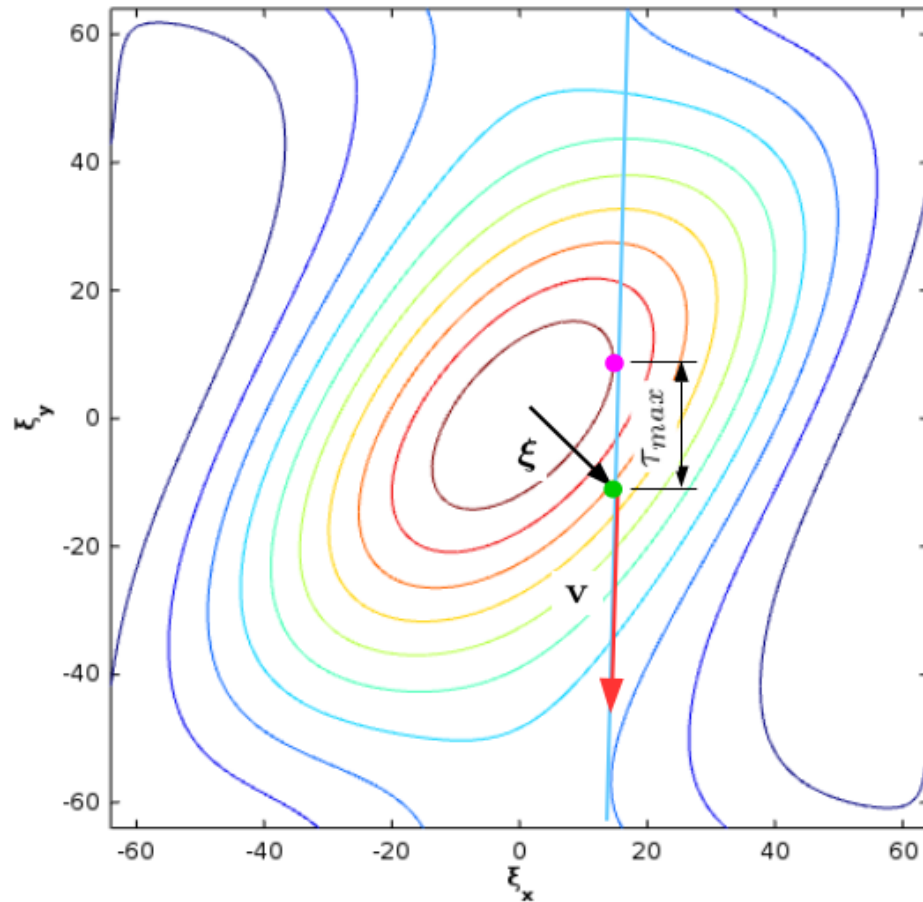
<

$$\tau_{\alpha}$$



Correlation function features recognition

$$C(\xi - \mathbf{v}\tau)$$



Briggs, B. H., On the analysis of moving patterns in geophysics, I, Correlation analysis, J. Atmos. Terr. Phys., 30, 1777-1788, 1968.

Estimation of geometry and drift velocity

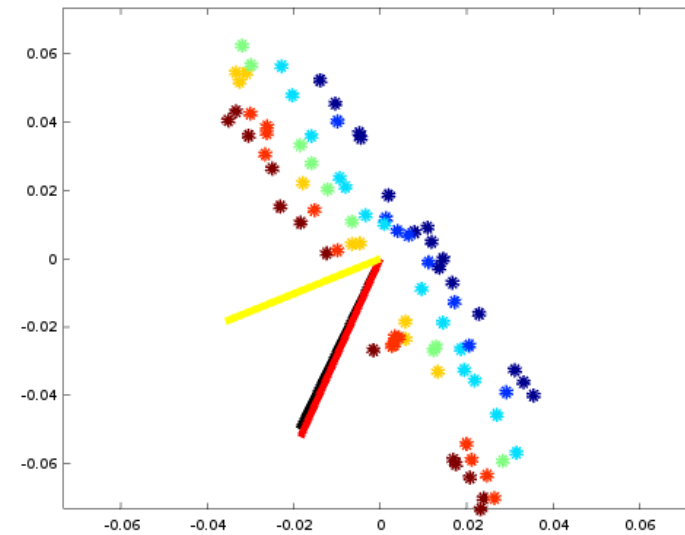
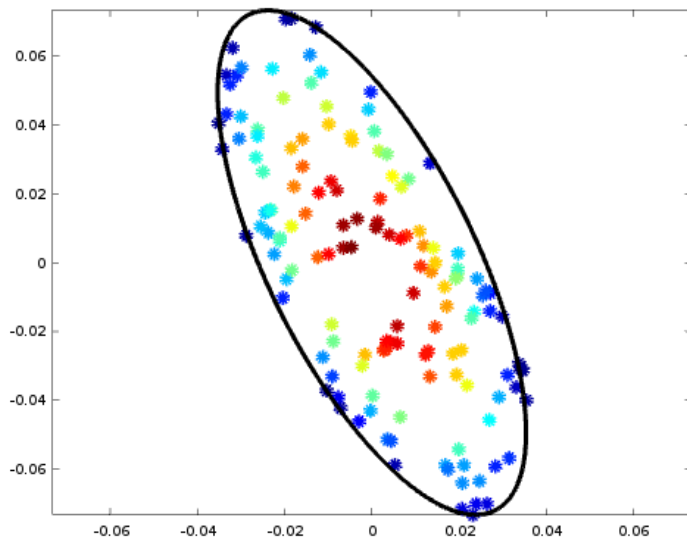
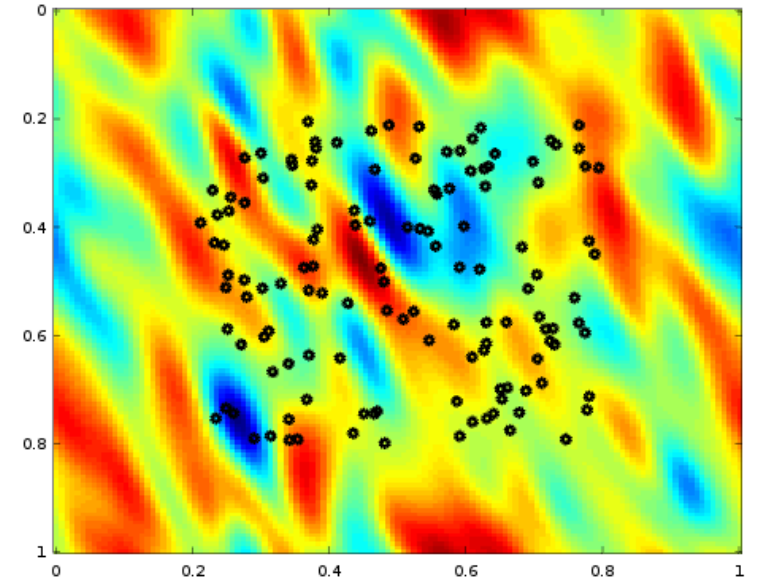
$$C(\boldsymbol{\xi}) = \rho(\boldsymbol{\xi}^T Q \boldsymbol{\xi})$$

$$\frac{\partial}{\partial \tau} C(\boldsymbol{\xi} - \mathbf{v}\tau) = 0$$

$$\boldsymbol{\xi}^T Q \mathbf{v} = \tau_m \mathbf{v}^T Q \mathbf{v} \rightarrow \tau_m = \frac{\boldsymbol{\xi}^T Q \mathbf{v}}{\mathbf{v}^T Q \mathbf{v}}$$

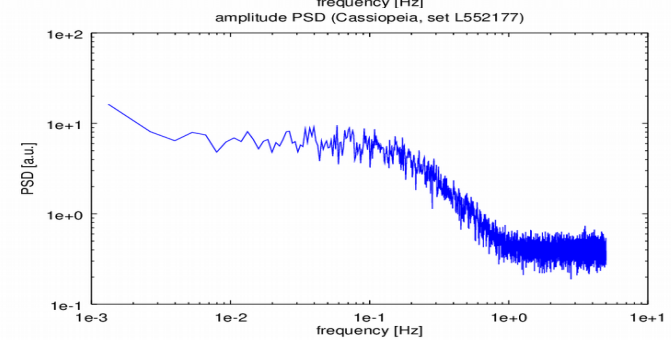
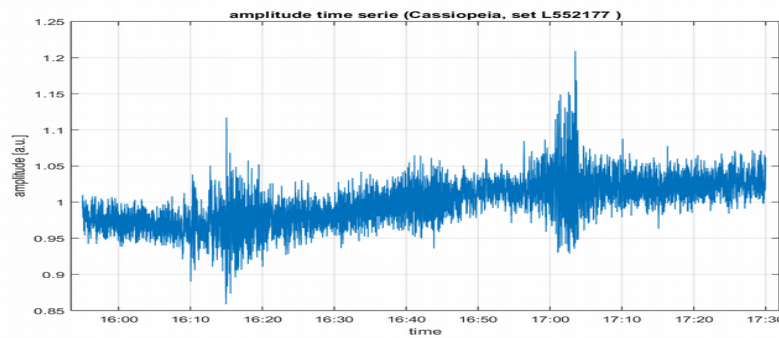
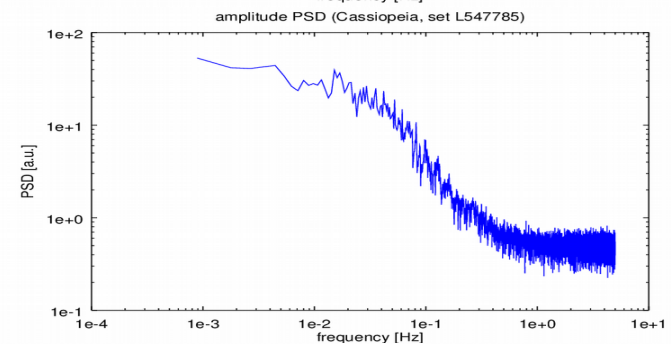
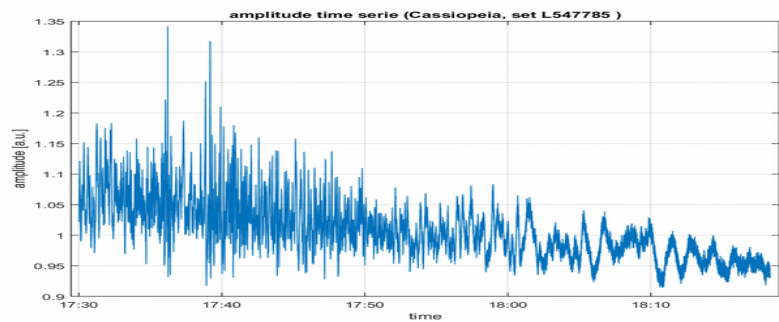
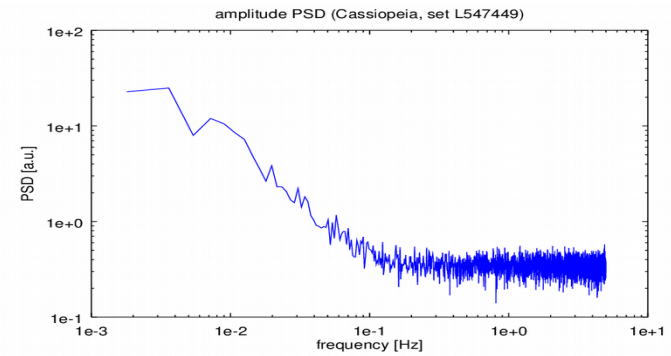
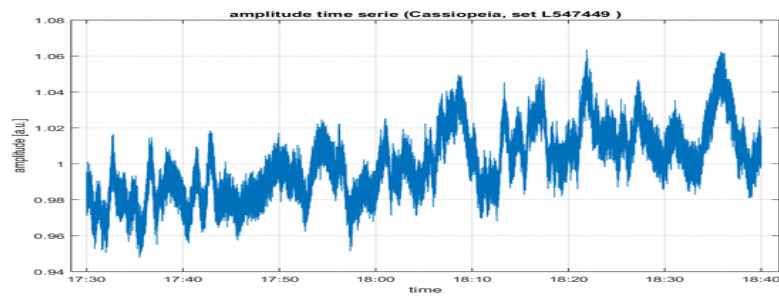
$$\nabla_{\boldsymbol{\xi}} \tau_m = \frac{Q \mathbf{v}}{\mathbf{v}^T Q \mathbf{v}}$$

$$\mathbf{v} = \frac{Q^{-1} \nabla_{\boldsymbol{\xi}} \tau_m}{(\nabla_{\boldsymbol{\xi}} \tau_m)^T Q^{-1} \nabla_{\boldsymbol{\xi}} \tau_m}$$

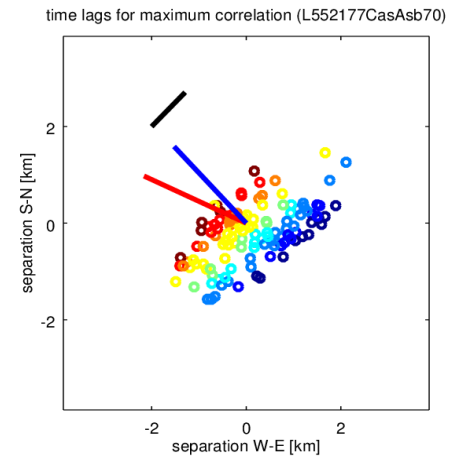
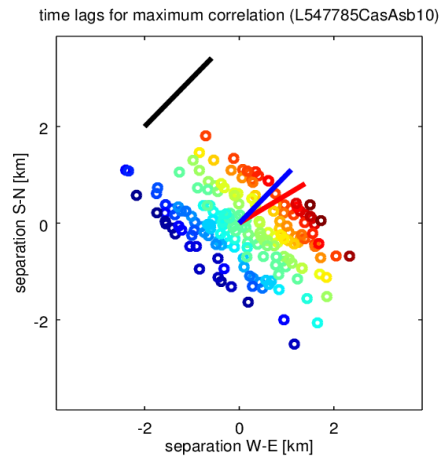
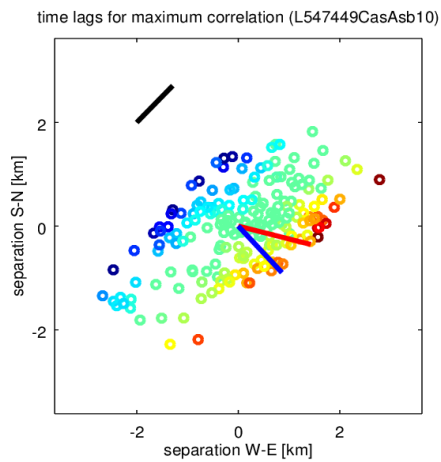
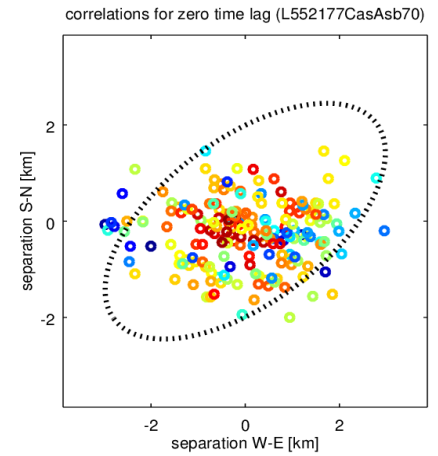
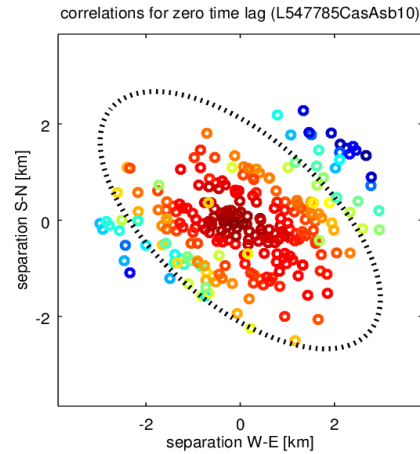
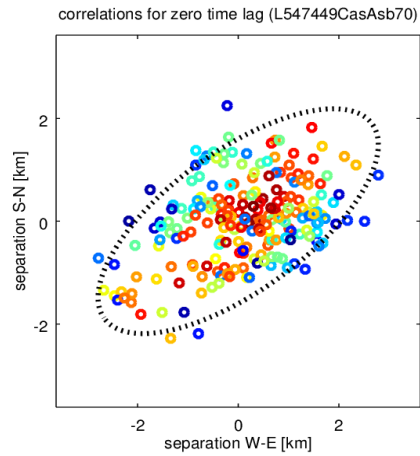


Some amplitude scintillation LOFAR data

data set	date & time of start	date & time of stop	short characteristics
L547449	2016-09-20 17:30:00	2016-09-20 18:40:00	quiet
L547785	2016-09-25 03:30:00	2016-09-25 06:55:00	small disturbance
L552177	2016-10-13 15:55:00	2016-10-13 17:30:00	storm - main phase

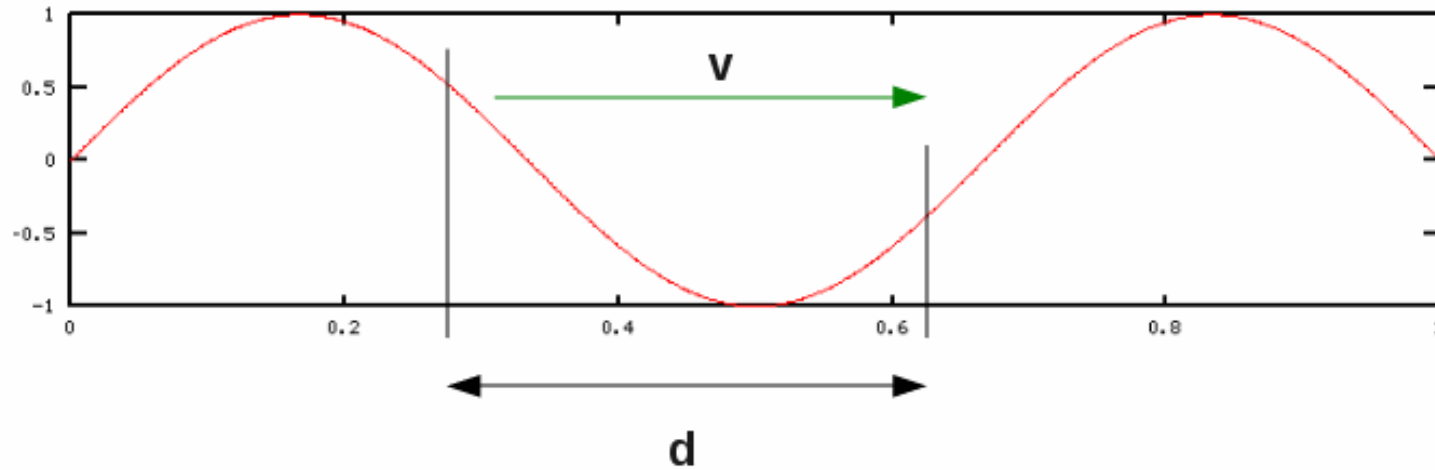


Estimation of geometry and drift velocity



data set	v_x [m/s]	v_y [m/s]	magnitude [m/s]	v_x isotropic [m/s]	v_y isotropic [m/s]	magnitude isotropic [m/s]
L547449	142	-35	147	86	-90	124
L547785	694	408	804	549	552	778
L552177	-2160	795	2370	-1526	1586	2200

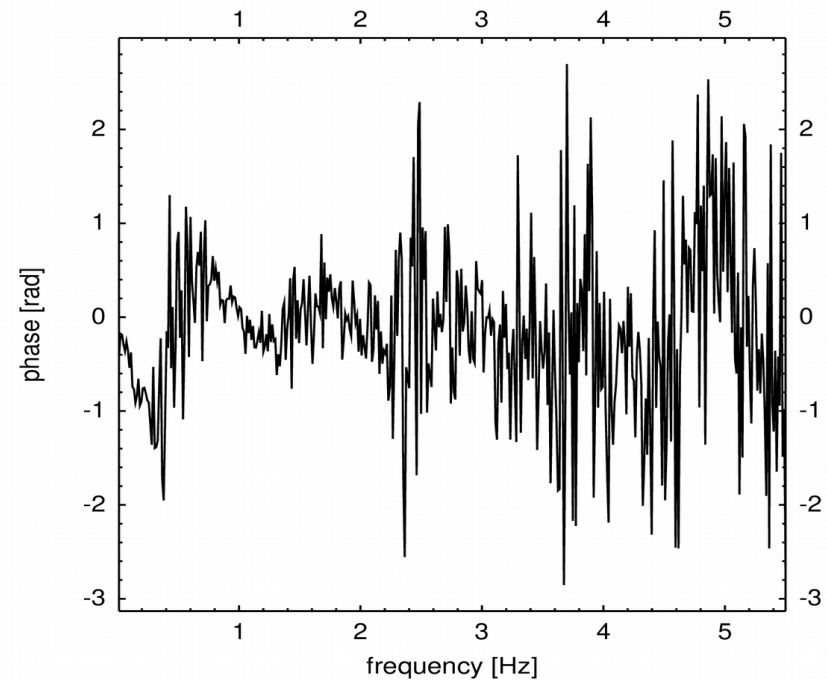
Space-frequency analysis



$$f = \exp ikx \quad x \rightarrow x - vt$$

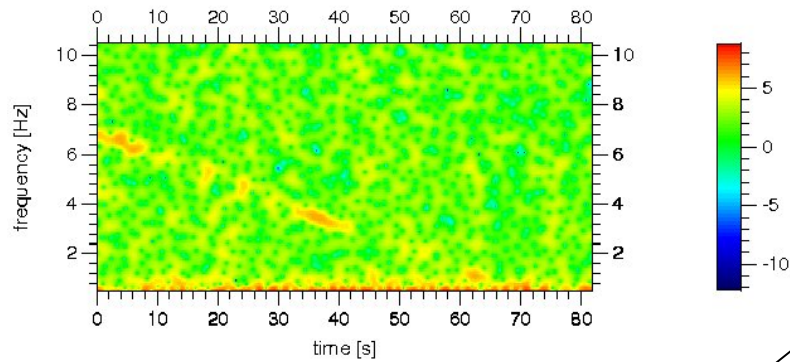
$$f(x_1, t_1)f^*(x_2, t_2) = \exp(ikd)\exp(ikv\tau), \quad d = x_1 - x_2, \quad \tau = t_1 - t_2$$

$$\omega = kv, \quad \Delta\phi = kd \rightarrow \Delta\phi = \frac{d}{v}\omega$$

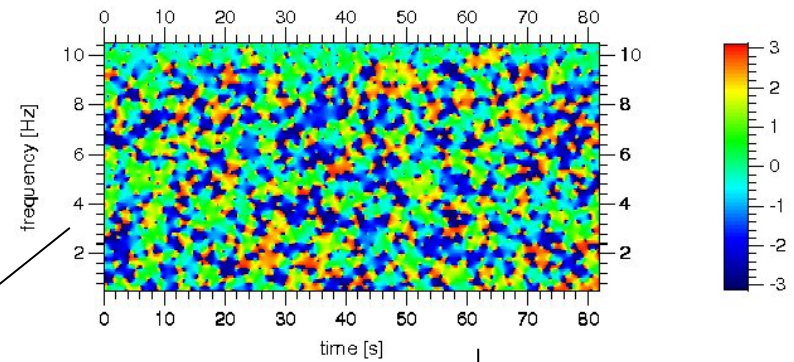


Space-frequency analysis cont.

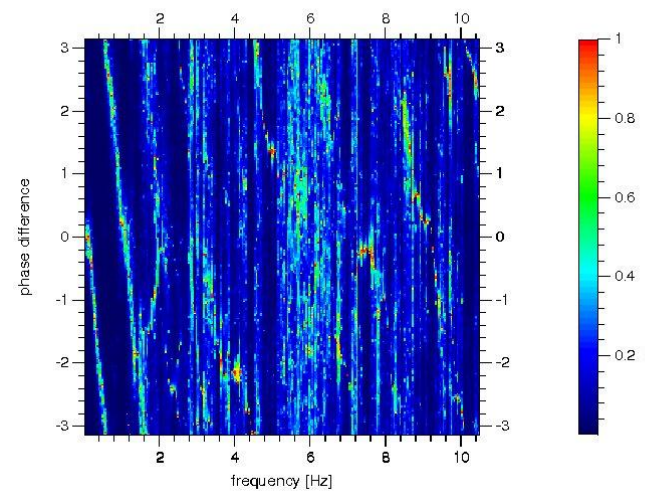
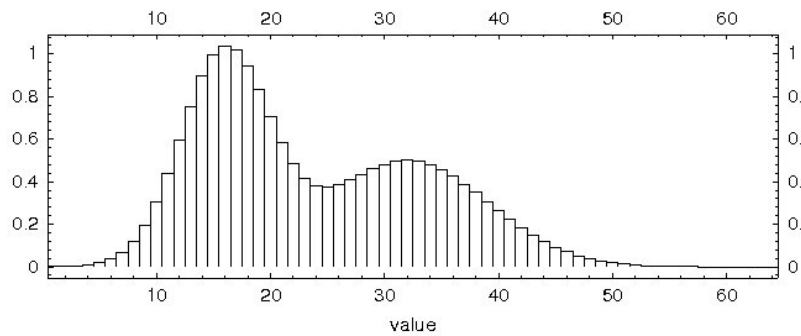
windowed fourier power



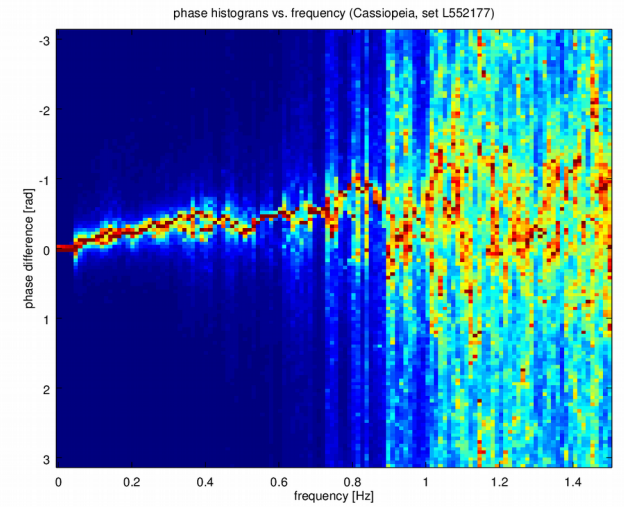
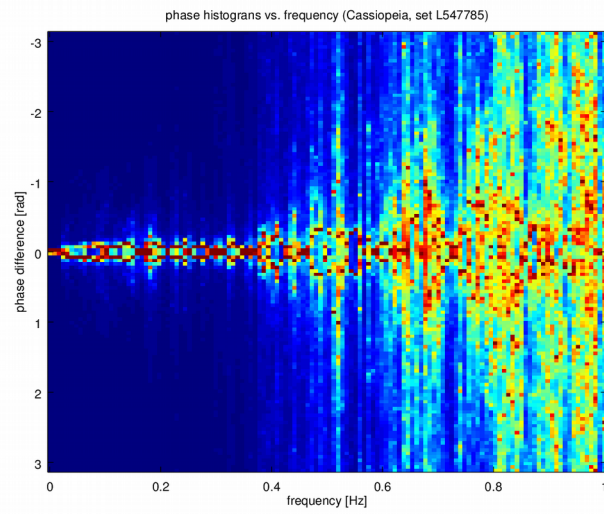
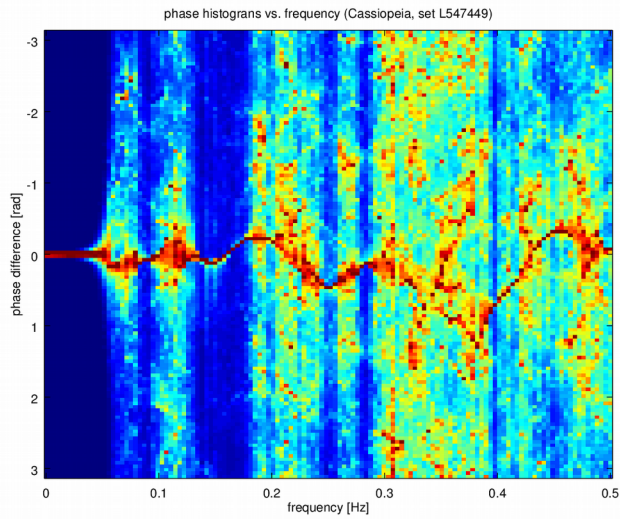
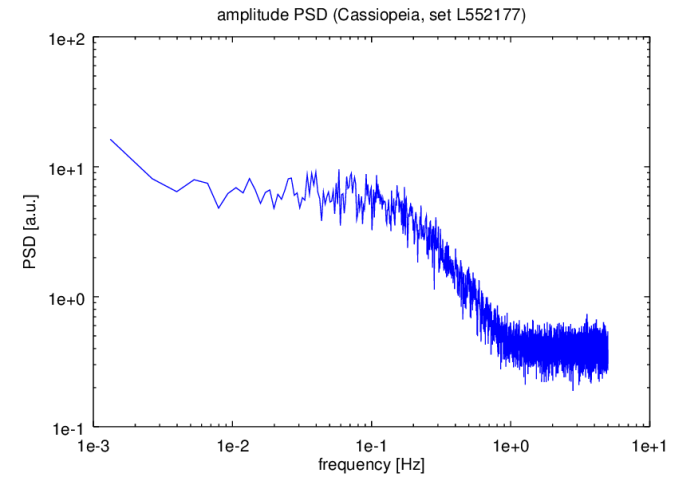
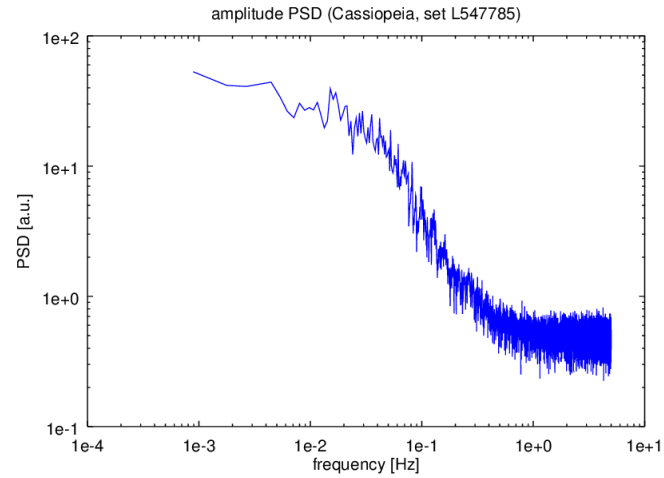
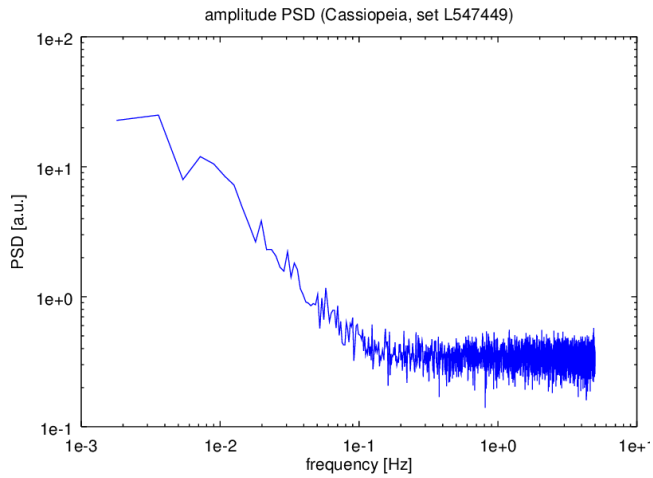
windowed fourier phases



Phase difference histograms

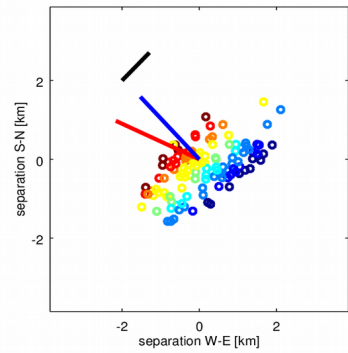


Frequency domain picture (dispersion)

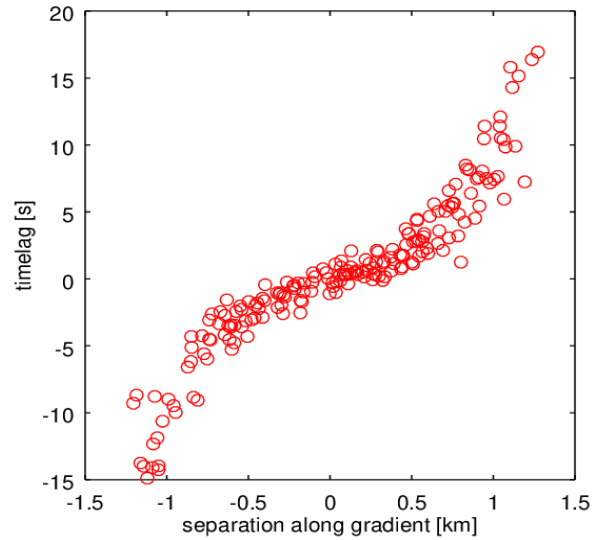


Time vs. frequency

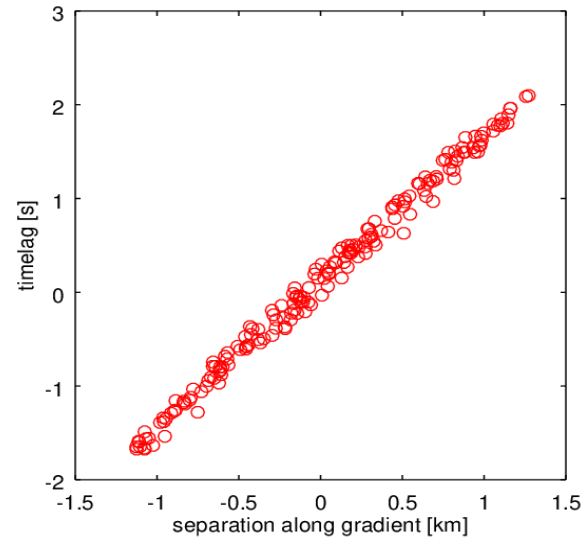
time lags for maximum correlation (L552177CasAsb70)



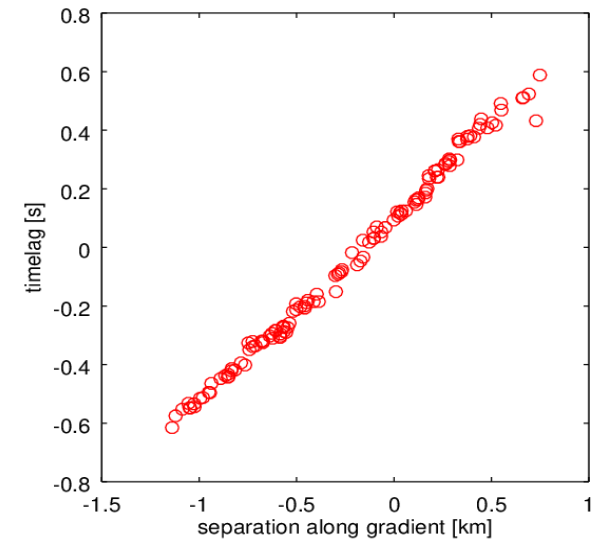
time lags for maximum correlation (L547449CasAsb10)



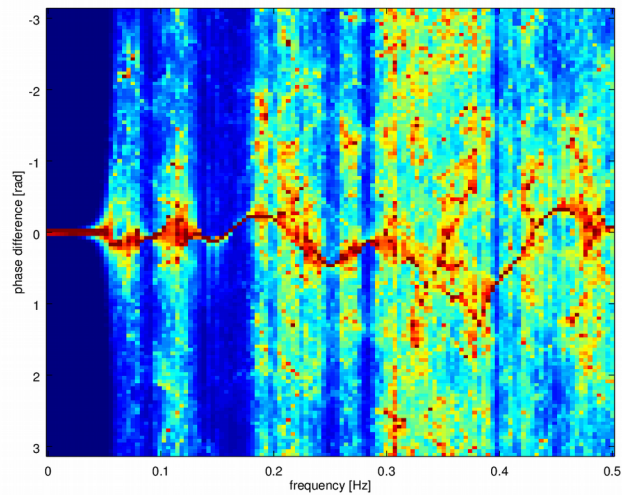
time lags for maximum correlation (L547785CasAsb10)



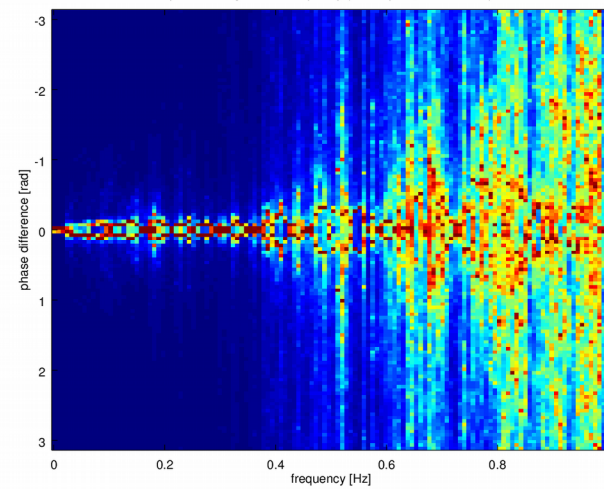
time lags for maximum correlation (L552177CasAsb70)



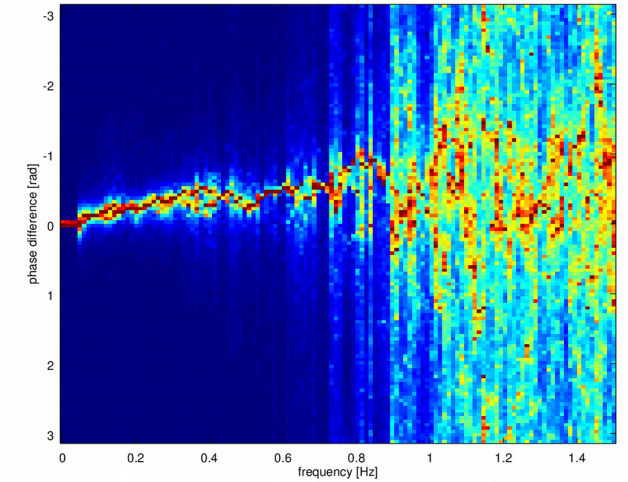
phase histograms vs. frequency (Cassiopeia, set L547449)



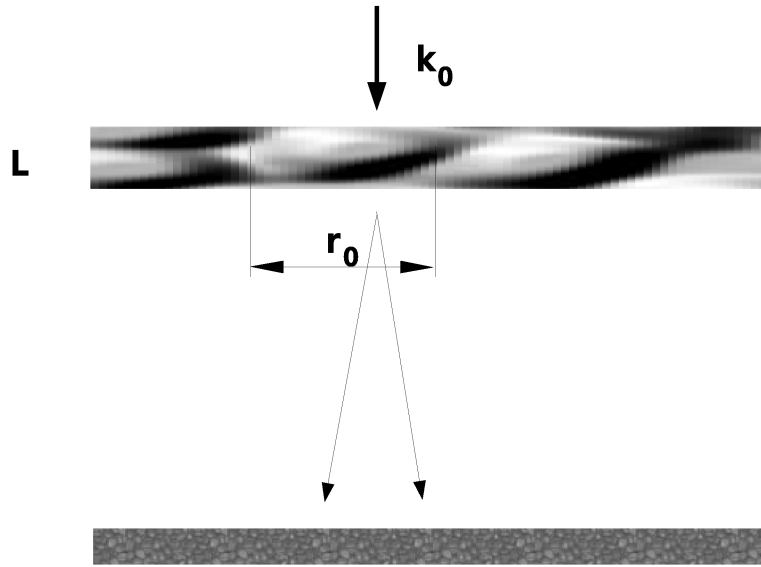
phase histograms vs. frequency (Cassiopeia, set L547785)



phase histograms vs. frequency (Cassiopeia, set L552177)



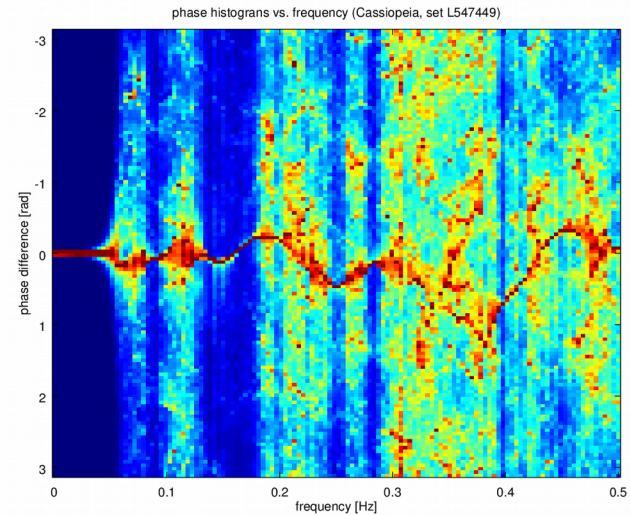
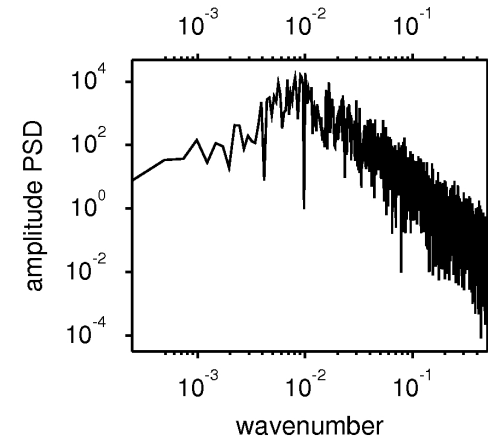
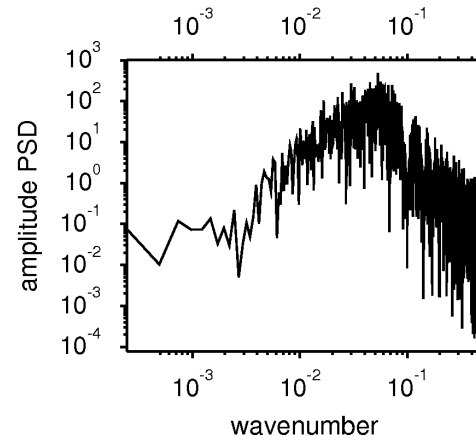
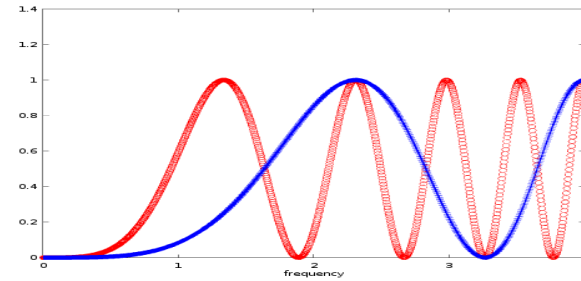
Phase screen approach & Fresnel filtering



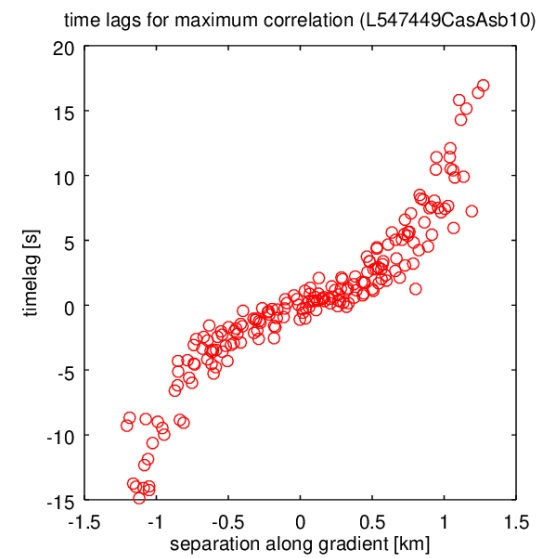
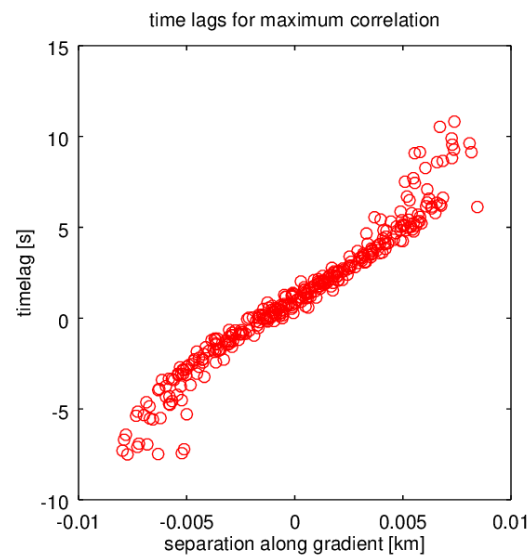
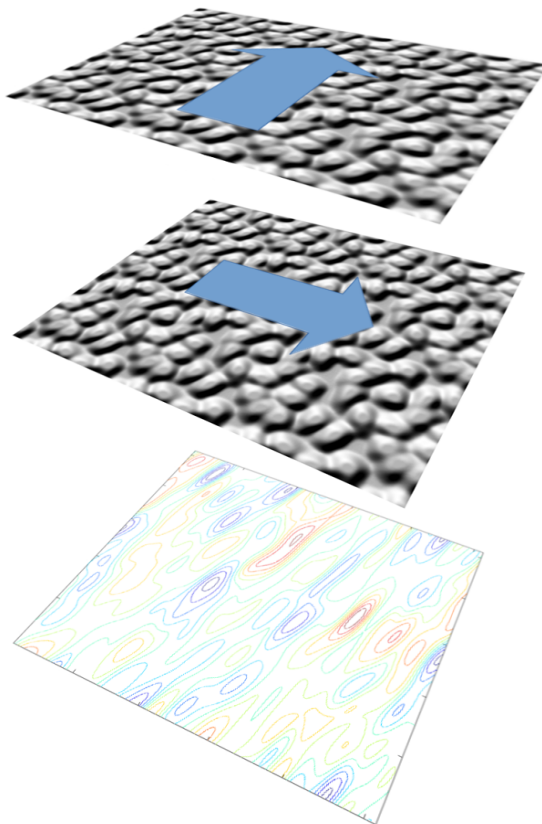
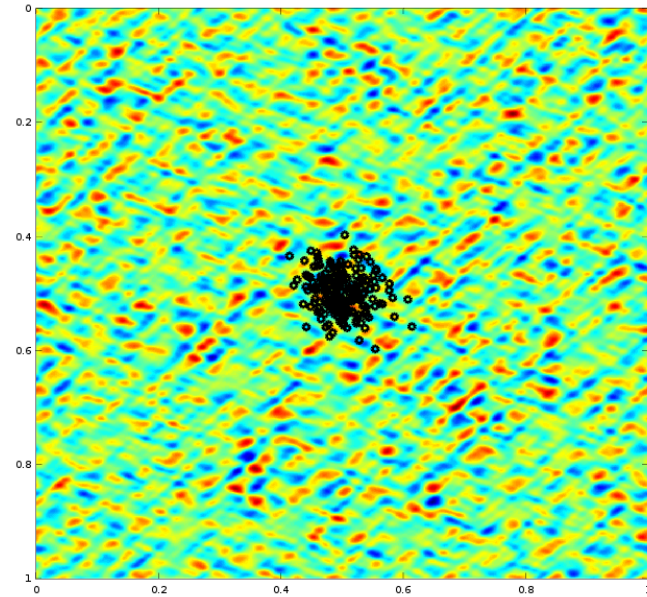
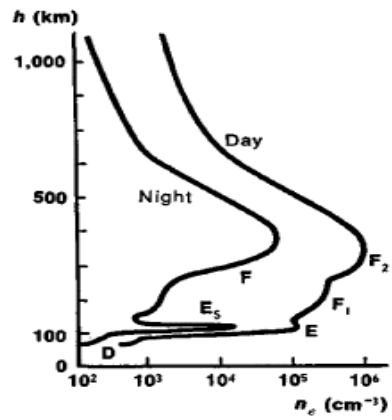
$$\sqrt{\lambda L} \ll r_0$$

$$u(\mathbf{r}_\perp, z) = u_0 \frac{ik_0}{2\pi z} \int d\mathbf{r}'_\perp \exp \left[-i \left(\frac{k_0(\mathbf{r}_\perp - \mathbf{r}'_\perp)^2}{2z} + \delta\phi(\mathbf{r}'_\perp) \right) \right]$$

$$\delta\phi(\mathbf{r}_\perp) = -r_e \lambda \int dl \Delta N_e(\mathbf{r}_\perp, l)$$



Double phase screen



Conclusions

LOFAR network provides consistent scintillation data of coverage both in time and space that equips us with new possibilities of spatio-temporal analysis.

The method presented gives estimate of drift velocity taking into account possible anisotropy of irregularities. It turns out that the magnitude of drift velocity depends on geomagnetic activity: the larger Kp index the greater velocity which is in agreement with previous observations.

Similar scales of irregularities revealed by correlation analysis at given time instant in conjunction with velocity estimates explain broadening of frequency power spectra - larger drift velocity shifts spatial structures in frequency domain according to the Doppler effect.

Observed nonlinear dependence of time lag on separation can be attributed to propagation through multilayer ionosphere with different evolution properties.